A Thermal Cycling Route for Processing Nano-grains in AISI 316L Stainless Steel for Improved Tensile Deformation Behaviour

Tarun Nanda[*], B. Ravi Kumar[#], and Vishal Singh[@]

[*]Department of Mechanical Engineering, Thapar University, Patiala - 147 004, India
[#]MST Division, National Metallurgical Laboratory, Jamshedpur - 831 007, India
[@]Department of Mechanical Engineering, Indus International University, Una - 174 301, India
[*]E-mail:tarunnanda@thapar.edu

ABSTRACT

The present work significantly improved the mechanical strength of AISI 316L stainless steel by producing nano-sized grains. Steel was subjected to cold rolling followed by repetitive thermal cycling to produce ultra-fine/nano-sized grains. The optimum processing parameters including extent of cold deformation, annealing temperature for thermal cycling, soaking period during each thermal cycle, and number of thermal cycles were determined through a systematic step-by-step procedure. After conducting thermal cycling under optimum conditions, a significant amount of grain size reduction was achieved. The effect of nano-sized grains on tensile deformation behavior was analysed. High cold deformation resulted in increased amount of stored strain energy. The stored strain energy accelerated the re-crystallisation kinetics during the thermal cycling process. Every thermal cycle resulted in irregular dispersal of stored energy. This irregular dispersal of stored energy favoured recrystallisation rather than grain growth and led to refinement of grains, in the absence of strain induced martensite. Repetitive thermal cycling promoted grain refinement and resulted in very significant grain size reduction with resultant grain size in the range of 800–1200 nm as compared to initial size of 90–120 μm. The resultant microstructure improved tensile strength by 106.8 per cent, from 590 MPa to 1220 MPa.

Keywords: Thermal cycling, dislocation-density, recrystallisation, cold deformation, stainless steel, strained-induced-martensite

1. INTRODUCTION

AISI 316L austenitic stainless steels are widely applicable in industry due to their excellent formability, corrosion resistance, and good weld-ability[1–3]. However, application of this material is restricted due to its low yield strength[4,5]. As per the Hall-Petch relationship, material's strength can been hanced by reducing its grain size[6,7]. Several techniques like plastic deformation and/or subsequent recrystallisation, cold rolling followed by severe plastic deformation (SPD) etc. have been employed by researchers for grain refinement of austenitic stainless steels[8,9]. Researchers have also focused on formation of nano-sized grains in considerably metastable austenitic stainless steels in the presence of strain induced martensite (SIM)[10–13]. It is reported that cold deformation followed by thermal cycling process slows down the grain growth and increases the re-crystallisation kinetics[13, 14].

The present research work was an attempt to produce nano-sized grains in a stable AISI 316L austenitic stainless steel, without formation of strain induced martensite in the steel. Heavy cold rolling followed by repetitive thermal cycling was employed to produce ultra-fine/ nano-sized grains in the steel. Further, the effect of these nano-grains on the tensile properties of AISI 316L steel was also investigated.

1.1 Cold Deformation and Dislocation Density

Cold deformation is directly related with dislocation density. Further, high dislocation density is related to stored strain energy[15]. High amount of stored energy accelerates the kinetics of recrystallisation. Hence, evaluation of stored energy i.e. dislocation density is highly desired to understand the re-crystallisation behaviour during the annealing process. The dislocation density) (ρ) of stainless steel is related with amount of cold deformation using Eqn. (1)[16].

$$\sigma = \sigma_0 + \alpha\mu b\rho^{-1/2} \tag{1}$$

where σ is the flow stress after cold deformation, σ_0 is the initial flow stress of 210 MPa, α is a constant of the order of 0.5, μ is shear modulus of 80 GPa and b is burger vector of 2.49Å, respectively for austenitic stainless steel[17,18]. The mathematical model of *Ludwigson* to relate the flow stress to strain for austenitic stainless steel is given as Eqn. (2)[19,20].

$$\sigma = K\varepsilon^n + \exp\left(K_1 + n_1\varepsilon\right) \tag{2}$$

where K, n, K_1 and n_1 are constants of *Ludwigson's* relation. The flow curve parameters derived for austenitic stainless steel in *Ludwigson's* work are given as: K= 1356 MPa; n= 0.453; K_1= 5.2 and n_1= 19.3[19,20].

Further, the effect of cold deformation on dislocation density can be estimated using linear *Bailey-Hirsch* relationship as shown in Eqn. (3)[21].

$$HV[GPa] = 0.7 + 3\times10^{-8}\rho^{1/2} \tag{3}$$

where HV is the Vickers hardness (GPa) and ρ is the dislocation density (m^{-2}).

1.2 Fraction of Re-crystallisation

Dischino[22], *et al.* used Eqn. (4) to evaluate the re-crystallisation fraction (X) under different annealing conditions.

$$X = \frac{H_0 - H_t}{H_0 - H_a} \qquad (4)$$

where H_0, H_t, and H_a, are the hardness values of cold deformed structure, annealed material in time (t), and the solution annealed material. Also, re-crystallisation kinetics can be described by JMAK relation as given by Eqn. (5)[23–27].

$$X = 1 - e^{(-kt^n)} \qquad (5)$$

where X is re-crystallised fraction (in time period t), n is the strain hardening exponent and k is a constant which depends upon temperature as shown in Eqn. (6)[23–27].

$$k = k_0 e^{(-Q/RT)} \qquad (6)$$

where k_0 is a constant of 0.225×10^2, Q is the activation energy of 177 kJ/mol for stainless steel, R is gas constant, and T is the absolute annealing temperature[28].

2. MATERIALS AND METHODS

AISI 316L grade of austenitic stainless steel in hot rolled condition was used in the present work. Composition of starting material is presented in Table 1. To achieve chemical homogeneity, starting material was annealed at 1060 °C for 1 h followed by water quenching.

Table 1. Chemistry of starting AISI 316L steel

Element	C	Si	Mn	P	Cr	Ni	Mo	Fe
% wt.	0.025	0.30	1.20	0.030	16.90	10.60	2.06	Balance

Solution annealed specimens were subjected to multi-pass unidirectional cold rolling for different thickness reductions from 20 per cent – 90 per cent in steps of 10 per cent reduction per pass. To find the optimum temperature for thermal cycling, cold rolled specimens of size $10 \times 10 \times 1$ mm were initially subjected to isothermal annealing. For this, samples were heated to different annealing temperatures in the range of 700 °C – 950 °C (in intervals of 25 °C), were soaked here for 1 min each, and then air cooled. In the present work, annealing temperature of 900 °C was selected for thermal cycling process. Further, to determine the soaking periods for different cycles during thermal cycling process, experiments were conducted at constant temperature of 900 °C with different soaking periods in the range of 15 s – 45 s with step of 5 s. To maintain uniform temperature over the entire thickness of the sample, a soaking period of 15 s was estimated by using the method proposed by

Gao[29], *et al.* Experiments resulted in a soaking time period of 35 s for each cycle during the thermal cycling process. Figure 1 gives a brief description of the repetitive thermal annealing process followed in the present work.

Micro-hardness measurement (Leica VMHTAUTO, Lieca Microsystems; Germany) was conducted with indentation load, indenter speed, and dwell time as 50 g-force, 30 μm/s and 10 s, respectively. An average of ten values of hardness was taken for the fully recrystallised specimen and the cold deformed specimens, respectively. However, for specimens annealed under different processing conditions, microhardness (H_t) was determined by taking average of more than 20 hardness measurements. This large number of measurements for each specific processing condition helped in minimising errors due to local variations. For optical microscopy, the polished specimens were etched using a solution of concentrated HCl (9 ml) - concentrated HNO_3 (3 ml) and CH_3OH (4 ml). These were analysed using an optical microscope (Leica DM2500 M, Lieca Microsystems; Germany). Further, for detailed microstructural analysis, transmission electron microscope (JEOL JEM 2200FS, JEOL; USA) on some selected specimens at an operating voltage of 200 kV, was used to examine the microstructural changes at high resolution. Thin foils from the specimens were prepared by initial careful mechanical thinning. Subsequently final thinning for electron beam transparency was achieved by electro-polishing using a bath of acetic acid and 10 per cent Perchloric acid. Room temperature tensile testing was conducted on standard dog-bone shaped specimens (ASTM: E–8M standard, 25 mm gauge length) using a tensile testing machine (8862 High Precision Electric Actuator System, Instron, Norwood, USA) of 100 kN capacity with 1.3×10^{-4} s^{-1} as the strain rate.

3. RESULTS AND DISCUSSION

3.1 Solution Annealing

Solution annealing of the as-received AISI 316L sample resulted in a microstructure comprising of polygonal grains along with annealing twins as shown in Fig. 2. The average grain size of solution treated sample as found using linear intercept method was in the range of 90 μm – 120 μm.

3.2 Cold Deformation

Equation (1) was used to obtain the variation of dislocation density (ρ) with different stress levels (σ). Further, Eqn. (2) had given the variation in true stress of austenitic stainless steel (σ) as a function of strain (ε). Thus, using Eqns. (1) and (2), the effect of percent cold deformation on dislocation density was calculated. Figure 3(a) shows the effect of cold deformation on the micro-hardness of specimens. For practical confirmation of results obtained through Eqn. (1), the values of hardness
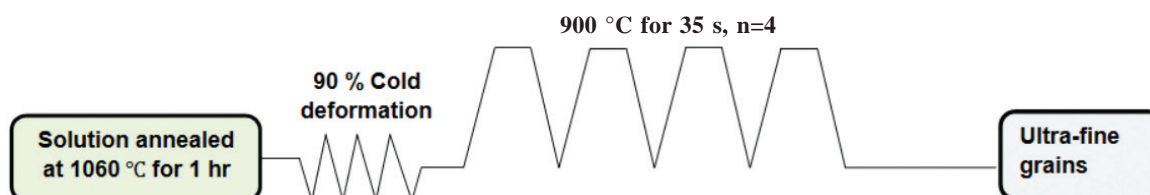

900 °C for 35 s, n=4

90 % Cold deformation

Solution annealed at 1060 °C for 1 hr

Ultra-fine grains

Figure 1. Graphical representation of the thermal cycling process. n = number of thermal cycles.
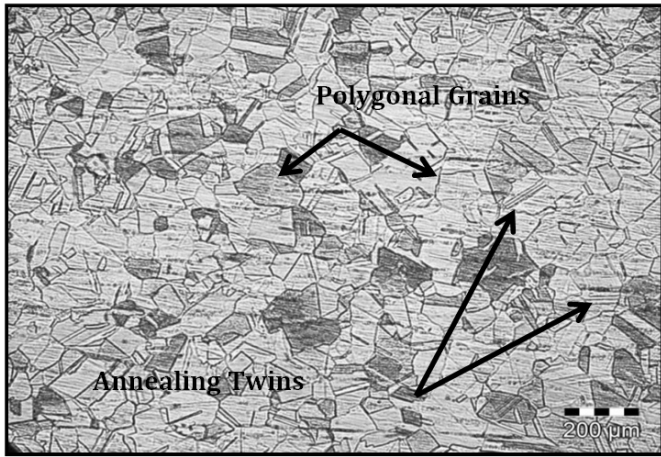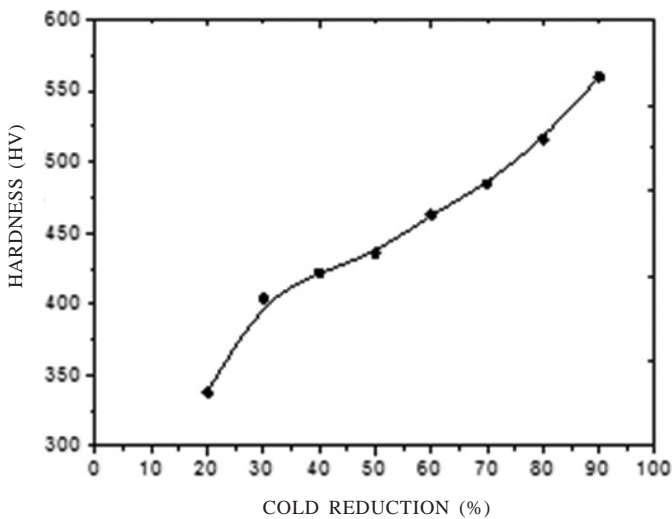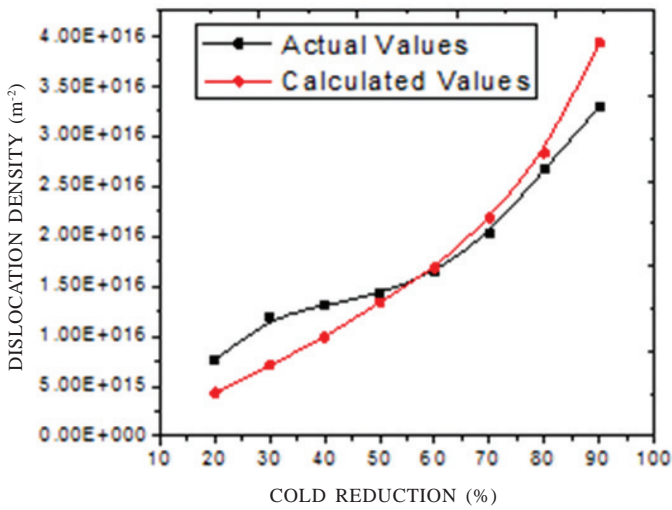
Figure 2. Optical micrograph of the solution treated 316L austenitic stainless steel.

(a)

(b)

Figure 3. Effect of cold deformation on (a) hardness, and (b) dislocation density.

obtained from Fig. 3(a) were used in Eqn. 3. Figure 3(b) shows the comparison of actual dislocation density values (calculated by hardness measurement i.e. Eqn. (3)) with calculated values

from the empirical relation (Eqn. (1)). It was observed that dislocation density increases with increase in percent of thickness reduction.

As discussed earlier, high dislocation density is directly linked with high stored strain energy in the material, and it accelerates the recrystallisation kinetics. High recrystallisation is highly desirable to obtain small sized grains. In order to obtain maximum grain size reduction, specimens subjected to 90 per cent thickness reduction (maximum cold deformation in the present work) were selected for further processing in the present study.

### 3.3 Recrystallisation Temperature

To determine the annealing temperature for the thermal cycling process, the cold rolled samples were initially subjected to isothermal annealing. They were heated to annealing temperatures in the range of 700 °C – 950 °C (in intervals of 25 °C), soaked there for 1 min each, and finally air cooled. A short holding period of 1 min was selected mainly because of two reasons. Primarily, Kumar and Gujral[14] reported that during the thermal cycling annealing process, a short holding period at the peak temperature is desired (otherwise, it causes grain growth). Secondly, from an industrial annealing viewpoint, short soaking periods of about 1 min at the annealing temperature at generally recommended[13,28]. Microstructures showed highly dislocated region (or deformed structure) for isothermal annealing in the temperature range of 700 °C and a partially recrystallised region for isothermal annealing in the temperature range of 800 °C. However, for annealing at 900 °C, nearlyfull recrystallisation was observed in the material. Further rise in temperature caused an increase in the austenite grain size. Some selected micrographs are presented in Fig. 4, which show a clear difference in un-recrystallised (annealing at 700 °C), partially recrystallised (annealing at 800 °C), and fully recrystallised microstructures (annealing at 900 °C) obtained under different conditions.

It was revealed that even with short holding time periods (1 min) at a temperature of 900 °C, it was possible to get a fully recrystallised microstructure. During thermal cycling annealing process, a short holding period at the peak temperature is desired (otherwise, it causes grain growth)[14]. Thus, the entire thermal cycling process was conducted at this temperature of 900 °C.
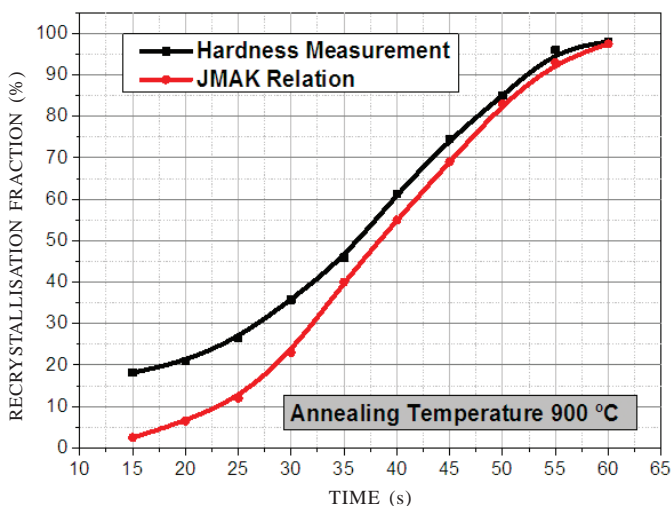
3.4 Recrystallisation Fraction

Cold rolled specimens with 90 per cent thickness reduction were now subjected to annealing treatment at 900 °C with different holding periods in a muffle furnace. The fraction of recrystallisation was calculated by using the measured hardness values in Eqn. (4). JMAK relation (Eqn. (5)) was also used to calculate the fraction of recrystallisation. Recrystallised fractions with respect to soaking time periods obtained through both the sources were similar and are shown in Fig. 5.

Figure 5 shows the actual volume of recrystallised fraction in the material corresponding to different soaking periods at a constant annealing temperature of 900 °C. It can be noted from Fig. 5 that nearly 50 per cent recrystallisation was complete for soaking time of about of 35 s. The present study involved
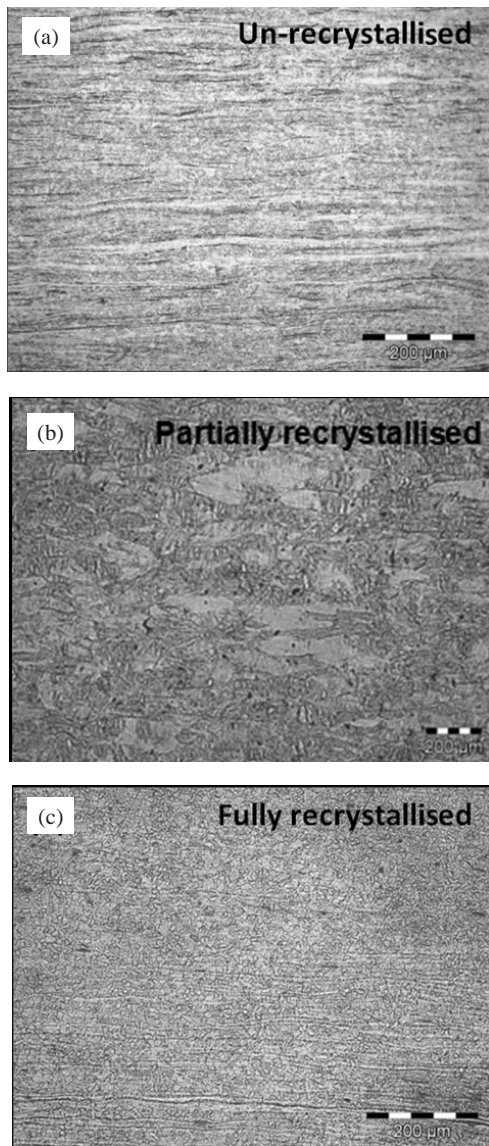
Figure 4. Optical image of 316L austenitic stainless steel after isothermal annealing at (a) 700 °C (b) 800 °C and (c) 900 °C

Figure 5. Recrystallisation fraction at 900 °C for different soaking periods.

a thermal cycling process that caused strain heterogeneity between the recrystallised portion and the cold deformed region during every thermal cycle. Further, it was desired to complete 50 per cent of recrystallisation in first thermal cycle and remaining 50 per cent in the subsequent thermal cycles. These conditions were being met for a soaking period of 35 s at 900 °C. Hence, a soaking time period of 35 s was selected for various thermal cycles.

3.5 Thermal Cycling

Thermal cycling was now conducted with the optimum annealing parameters i.e. at a constant annealing temperature of 900 °C with holding period of 35 s for all thermal cycles, as shown in Fig. 1. The numbers of thermal cycles were restricted to four as reported in an earlier work by Kumar and Gujral[14]. The authors had reported that with number of thermal cycles more than four, grain growth results and with number of cycles lesser than four, only partial recrystallisation occurs[14]. Thus, in the present work, for the thermal cycling process, the numbers of cycles were taken as four. Thereafter, for n = 4 (four thermal cycles), the optimum annealing temperature and soaking time period were determined for the thermal cycling process which could result in formation of ultra-fine grained structure for improved strength. In the present work, thermal cycling was conducted under various conditions before reaching the optimum conditions of 900 °C, 35 s, and n = 4. Some of these annealing conditions and the corresponding micrographs are shown in Fig. 6. Partial recrystallisation and grain growth can be observed for thermal cycling at 875 °C (Fig. 6(a)) and 925 °C (Fig. 6(b)) respectively with a constant soaking period of 35 s. Similarly, thermal cycling at 900 °C with soaking period of 30 s and 40 s resulted in partial recrystallisation and grain growth, respectively. A review of microstructures and also grain size measurement revealed that the sample thermal cycled at 900 °C for 35 s showed ultrafine grained structure (see Fig. 6(c). This microstructure showed fully recrystallised ultra-fine grains, while other microstructures gave an indication of either un-recrystallised region or occurrence of slight grain growth.

3.6 TEM Analysis Under Optimum Conditions

Figure 7 shows the Bright field TEM image of AISI 316L stainless steel sample after thermal cycling under the selected optimum processing conditions. From the above study, it was found that a suitable combination of annealing temperature, soaking time, and number of cycles (annealing at 900 °C for 35 s; 4 cycles) provide appropriate results in terms of grain size reduction. The TEM image showed a uniform distribution of recrystallised ultrafine strain free grains (< 1 μm) with a very small portion of grains with deformed structure (Fig. 7). Some grains with zigzag dislocations (marked with black arrow) and parallel slip lines (marked with white arrow) evidenced the presence of deformation effect. Average grain size of the finally processed specimen was in the range of 800 nm –1200 nm (using linear intercept method)[13,28].

3.7 Tensile Properties under Optimum Conditions

Figure 8 shows the tensile curves of the solution annealed and the thermal cycled specimens. Solution annealed specimen
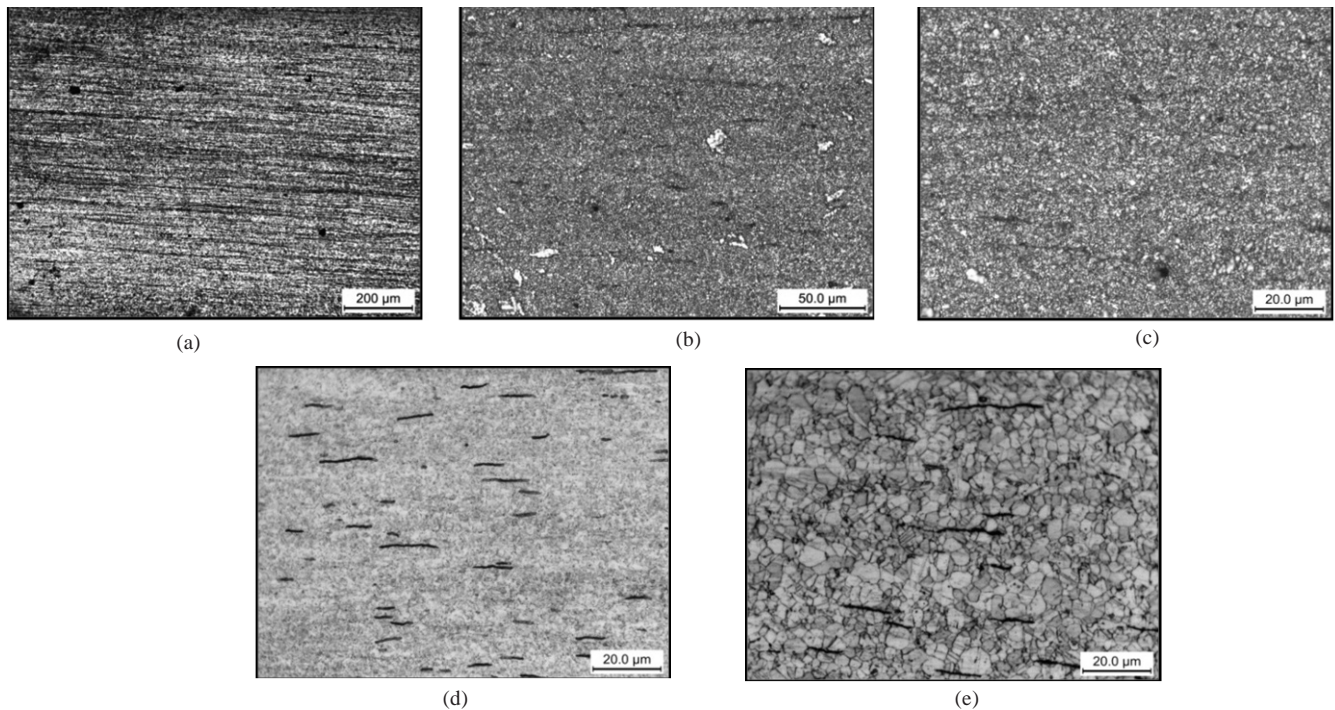
Figure 6. Microstructure of 316L austenitic stainless steel thermal cycled at different conditions (number of thermal cycles =4) (a) 875 °C, 35 s, (b) 925 °C, 35 s, (c) 900 °C, 35 s, (d) 900 °C, 30 s, (e) 900 °C, 40 s.
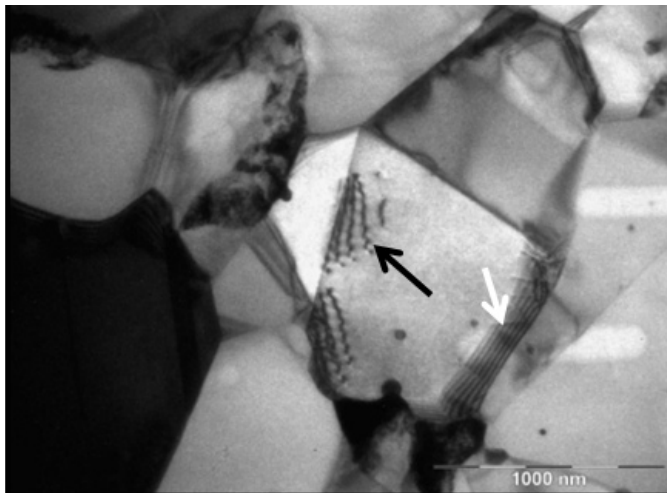

Figure 7. TEM images of AISI 316L stainless steel after thermal cycling under the optimum conditions.

Figure 8. Tensile curves of solution annealed and thermal cycled specimen of AISI 316L stainless steel.

resulted in low yield strength (YS = 268 MPa) and ultimate tensile strength (UTS = 590 MPa) which can be attributed to the presence of coarse grains. Specimen subjected to thermal cycling under the optimum conditions showed very high YS (1100 MPa) and UTS (1220 MPa). Further, the thermal cycled specimen resulted in almost negligible strain hardenability during tensile deformation in the plastic regime. The corresponding microstructure revealed presence of ultrafine/nano-sized grains, as shown in Fig. 7. These ultra-fine grains were also noted to contain some dislocations within the microstructure (Fig. 7).

The observed poor strain hardenability with increased YS and UTS in thermal cycled specimen was attributed to presence of nano-sized grains and that too containing some dislocations.
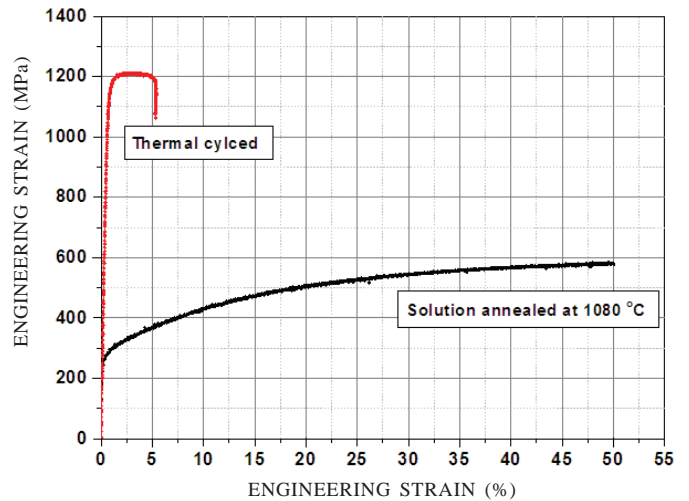
The combined effect of nano-sized grains with dislocations present in them were responsible for poor strain hardenability and ductility.

4. CONCLUSIONS

The present work investigated the grain refinement possibility of a stable austenitic stainless steel, AISI 316L. Stable austenitic stainless steels (ASS) do not undergo any phase transformation unlike their metastable counterparts in which formation of strain induced martensite (SIM) takes place. In the metastable austenitic stainless steels, presence of large volumes of SIM promotes nucleation rate and leads to grain refinement[16]. SIM reversion, (if present in large fraction) is considered to be the main reason for refinement of grain

size in metastable ASS. However, for stable type ASS, it is the heterogeneity in nucleation and grain growth behaviour that is responsible for grain refinement in the absence of transformation to SIM. This heterogeneity is a function of cold deformation followed by thermal cycling. In the present work, a thermal cycling processing route was developed for formation of ultrafine grained AISI 316L in the absence of SIM transformation. The tensile properties of the thermal cycled nano/ ultrafine grained steel provided high yield and ultimate tensile strength as compared to the solution annealed specimen. During the initial few thermal cycles, nucleation took place in areas with high strain energy i.e. highly deformed areas. This caused strain heterogeneity between the newly re-crystallised and the remaining un-recrystallised regions. After every thermal cycle, strain heterogeneity increased and resulted in irregular dispersal of stored energy. This irregular dispersal of stored energy during each thermal cycle favored recrystallisation against grain growth and thus led to refinement of grain size.

REFERENCES

1. Li,Y.; Hu, S.; Shen, J. & Hu, B. Dissimilar welding of H62 brass-316L stainless steel using continuous-wave Nd:YAG laser. *Mater. Manuf. Process.,* 2014, **29**(8), 916–21.
   doi:10.1080/10426914.2013.822981

2. Rao, G.A.; Sankaranarayana, M. & Balasubramaniam, S. Hot isostatic pressing technology for defence and space applications. *Def. Sci. J.*, 2012, **62**(1), 73–80.
   doi:10.14429/dsj.62.372

3. Sugur, V.S. & Manwani, G.L. Problems in storage and handling of red fuming nitric acid. *Def. Sci. J.*, 1983, **33**(4), 331–37.
   doi: 10.14429/dsj.33.6188

4. Eskandari, M.; Najafizadeh, A. & Kermanpur, A. Effect of strain-induced martensite on the formation of nanocrystalline 316L stainless steel after cold rolling and annealing. *Mat. Sci. Eng. A,* 2009, **519**, 46–50.
   doi: 10.1016/j.msea.2009.04.038

5. Ganesh, K.C.; Vasudevan, M.; Balasubramanian, K.R.; Chandrasekhar, N. & Vasantharaja, P. Thermo-mechanical analysis of TIG welding of AISI 316LN stainless steel. *Mater. Manuf. Process.,* 2014, **29**(8), 903–09.
   doi:10.1080/10426914.2013.872266

6. Mishnev, R.; Shakhova, I.; Belyakov, A. & Kaibyshev, R. Deformation microstructures, strengthening mechanisms, and electrical conductivity in a Cu–Cr–Zr alloy. *Mat. Sci. Eng. A*, 2015, **629**, 29–40.
   doi:10.1016/j.msea.2015.01.065

7. Rao, K.S. & N, Hossein. Brittle failure in heterogeneous crystalline rocks. *Def. Sci. J.*, 2008, **58**(2), 285–94.
   doi: 10.14429/dsj.58.1648

8. Ucok, I.; Ando, T. & Grant, N.J. Property enhancement in type 316L stainless steel by spray forming. *Mat. Sci. Eng. A*, 1991, **133**, 284–87. doi:10.1016/0921-5093(91)90070-4

9. Ye, K.L.; Luo, H.Y. & Ly, J.L. Producing nano-structured 304 stainless steel by rolling at cryogenic temperature. *Mater. Manuf. Process.*, 2014, **29**(6), 754–58.
   doi:10.1080/10426914.2014.901534

10. Kumar, B.R.; Das, S.K.; Mahato, B. & Ghosh, R.N. Role of strain-induced martensite on microstructural evolution during annealing of metastable austenitic stainless steel. *J. Mater. Sci.,* 2009, **45**, 911–18.
    doi: 10.1007/s10853-009-4020-8

11. Mythili, R.; Saroja, S. & Vijayalakshmi, M. Study of strain induced martensite formation in a Ti modified 316 stainless steel bellow by transmission electron microscopy. *T. Indian I. Metals*, 2009, **62**(6), 573–79.
    doi: 10.1007/s12666-009-0096-8

12. Li, Y.; Bu, F.; Kan, W. &Pan, H. Deformation-induced martensitic transformation behaviour in cold-rolled AISI304 stainless steels. *Mater. Manuf. Process.,* 2013, **28**(3), 256–59.
    doi:10.1080/10426914.2012.667897

13. Kumar, B.R.; Mahato, B.; Sharma, S. & Sahu, J.K. Effect of cyclic thermal process on ultrafine grain formation in AISI 304L austenitic stainless steel. *Metall. Mater. Trans. A,* 2009, **40**, 3226–234. doi: 10.1007/s11661-009-0033-9

14. Kumar, B.R. & Gujral, A.Plastic deformation modes in mono- and bimodal-type ultrafine-grained austenitic stainless steel. *Metall. Micro. Analysis,* 2014, **3**(5), 397–07.
    doi: 10.1007/s13632-014-0152-6

15. Szpunar, J.A.; Narayanan, R. & Li, H. Computer model of recrystallisation texture in aluminium alloys. *Mater. Manuf. Process.*, 2007, **22**(7–8), 928–33
    doi:10.1080/10426910701451820

16. Chia, K.H.; Jung, K. & Conrad, H. Dislocation density model for the effect of grain size on the flow stress of a Ti–15.2 at per cent Mo alloy at 4.2–650K. *Mat. Sci. Eng. A,* 2005, **409**, 32–38.
    doi:10.1016/j.msea.2005.03.117

17. Raghavan, V. Materials science and engineering. PHI Learning Private Limited, India, 2004. 285 p.

18. Roucoules, C.; Pietrzyk, M. & Hodgson, P.D. Analysis of work hardening and recrystallisation during the hot working of steel using a statistically based internal variable model. *Mat. Sci. Eng. A,* 2003, **339**, 1–9.
    doi:10.1016/S0921-5093(02)00120-X

19. Samuel, K.G. & Rodriguez, P. On power-law type relationships and the ludwigson explanation for the stress-strain behaviour of AISI 316 stainless steel. *J. Mater. Sci.,* 2005, **40**, 5727–731.
    doi: 10.1007/s10853-005-1078-9

20. Samuel, E.I. & Choudhary, B.K. Universal scaling of work hardening parameters in type 316L (N) stainless steel. *Mat. Sci. Eng. A,* 2010, **527**, 7457–460.
    doi:10.1016/j.msea.2010.08.021

21. Nakashima, K.; Suzuki, M.; Futamura, Y.; Tsuchiyama, T. & Takaki, S. Limit of dislocation density and dislocation strengthening in iron. *Mater. Sci. Forum*, 2006, **503–504**, 627–32.
    doi: 10.4028/www.scientific.net/MSF.503-504.627

22. Dischino, A.; Kenny, J.M.; Salvatori, I. & Abbruzzese, G. Modelling primary recrystallisation and grain growth in a low nickel austenitic stainless steel. *J. Mater. Sci.,* 2001, **36**, 593–01.

doi: 10.1023/A:1004856001632

23. Kolmogorov, A.N. On the statistical theory of crystallisation of metals (translated title). *Izv. Akad. Nauk. SSSR, 1937*, **1**, 355–59.

24. Avrami, M. Kinetics of phase change I. General theory. *J. Chem. Phys.,* 1939, **7**(12), 1103–109. doi: 10.1063/1.1750380

25. Johnson, W.A. & Mehl, R.F. Reaction kinetics in processes of nucleation and growth. *AIMMPE*, 1939, **135**(8), 416-442.

26. Avrami, M. Kinetics of phase change II. Transformation-time relations for random distribution of nuclei. *J. Chem. Phys.,* 1940, **8**(2), 212–24. doi: 10.1063/1.1750631

27. Avrami, M. Kinetics of phase change III. Granulation, phase change, and microstructure. *J. Chem. Phys.,* 1941, **9**(2), 177–84. doi: 10.1063/1.1750872

28. Kumar, B.R.; Das, S.K.; Sharma, S. & Sahu, J.K. Effect of thermal cycles on heavily cold deformed AISI 304L austenitic stainless steel. *Mater. Sci. Eng. A,* 2010, **527**, 875–82. doi: 10.1016/j.msea.2009.08.075

29. Gao, M.; Reid, C.N.; Jahedi, M. & Li, Y. Estimating equilibration times and heating/cooling rates in heat treatment of work pieces with arbitrary geometry. *J. Mater. Eng. Perform.*, 2000, **9**(1), 62–71. doi: 10.1361/105994900770346295

CONTRIBUTORS

Dr Tarun Nanda is currently working as an Assistant Professor in Mechanical Engineering Department at Thapar University, Patiala, Punjab. His research areas include processing of advanced high strength steels, stainless steels, and polymer based nanocomposites.
In the current study, his contribution in providing introduction portion, problem formulation, and discussion of results.

Dr B. Ravi Kumar is currently working as a Principal Scientist in MST Division at CSIR-National Metallurgical Laboratory, Jamshedpur. His research interests include materials characterisation and testing, processing of ultra-fine/nano-grained materials for improved mechanical properties.
In the current study, his contribution in providing assistance in design of annealing experiments, analysis of results, and drawing of conclusions.

Mr Vishal Singh received his Master's in Production Engineering from Thapar University, Patiala, 2015. Currently, he is working as an Assistant Professor in Mechanical Engineering department at Indus International University, Una, Himachal Pradesh. His areas of interests include steel processing, production technologies, and composite materials.
In the current study, his contribution in providing assistance in conduct of experiments, characterisation, and testing.